PROCEEDINGS OF THE IAEA CONFERENCE ON THE USED OF ESOTOPES IN BIOLOGICAL DINITROGEN FIXATION. Vienna, November 21-25, 1977

IAEA-AG-92/10

USE OF ^{13}N IN STUDIES OF FIXATION OF DINITROGEN AND ASSIMILATION OF AMMONIUM BY CYANOBACTERIA

J.C. MEEKS*, C.P. WOLK, J. THOMAS**
MSU-ERDA Plant Research Laboratory

S.M. AUSTIN, A. GALONSKY
Cyclotron Laboratory and Department of Physics,
Michigan State University,
East Lansing, Michigan,
United States of America

Abstract

USE OF ^{13}N IN STUDIES OF FIXATION OF DINITROGEN AND ASSIMILATION OF AMMONIUM BY CYANOBACTERIA.

^{13}N ($t_{1/2}$ = 10 min) has been used to identify the initial products of assimilation of N_2 and NH_4^+ by intact filaments of a number of cyanobacteria and by heterocysts isolated from *Anabaena cylindrica*. Ammonium, the amide nitrogen of glutamine, and the α-amino nitrogen of glutamate, in that order, were the first observed products of fixation of $[^{13}N]N_2$. Amide-labelled glutamine was the initial product of metabolism of $^{13}NH_4^+$ by *A. cylindrica* grown with either NH_4^+ or N_2 as the nitrogen source. Glutamate was the second major product of $^{13}NH_4^+$ assimilation. Isolated heterocysts form [^{13}N]glutamine but not [^{13}N]glutamate from $[^{13}N]N_2$ or $^{13}NH_4^+$. Formation of [^{13}N]glutamine from $[^{13}N]N_2$ was inhibited by acetylene, indicating metabolic coupling of the activity of glutamine synthetase to that of nitrogenase in these cells. A diffusible substance produced by heterocysts inhibits nearby cells of the same filament from differentiating into heterocysts. Glutamine (or a derivative of glutamine) may be involved in inhibiting differentiation of vegetative cells.

INTRODUCTION

When grown in the absence of a source of combined nitrogen, vegetative cells of certain cyanobacteria (blue-green algae) differentiate into thick-walled cells termed heterocysts. A considerable amount of indirect [1–4] and direct [5, 6] evidence supports the idea that heterocysts are the major loci of N_2 fixation in filamentous, heterocyst-forming cyanobacteria under aerobic conditions.

---

* Permanent address: Department of Bacteriology, University of California, Davis, California.

** Permanent address: Biology and Agriculture Division, Bhabha Atomic Research Division, Trombay, Bombay, India.

INTERNATIONAL CONFERENCE ON NUCLEAR PHYSICS WITH ELECTROMAGNETIC INTERACTIONS, Mainz, Germany, June 5-9, 1979.

SHELL-MODEL INTERPRETATION OF INELASTIC ELECTRON SCATTERING TO STRONG 2^+ AND 4^+ STATES IN THE SD-SHELL

W. Chung and B. H. Wildenthal
Cyclotron Laboratory, Michigan State University, East Lansing, Michigan 48824

The form factors for electron scattering to the most strongly excited $J^\pi = 2^+$ and 4^+ states in ^{20}Ne, ^{24}Mg, ^{28}Si, ^{32}S and ^{36}Ar have been calculated in the Born approximation from shell-model wave functions obtained by diagonalizing the Chung-Wildenthal empirical effective Hamiltonians[1,2] in the full $d_{5/2}$-$s_{1/2}$-$d_{3/2}$ basis space. The radial dependences of the single-nucleon wave functions were assumed alternatively to be given by the harmonic oscillator and Saxon-Woods forms. The radius parameter were chosen to reproduce rms radii data.

The microscopic foundations for these excitations are the matrix elements of the $\Delta J=2, \Delta T=0$ matrix elements of the coupled annihilation and creation operators $a_{j'}$ and $a^\dagger_j$ for nucleons in the model orbitals $(nlj)'$ and (nlj). These are listed in Table 1. The collectiveity of the 2^+ excitations stems from the relative phases of the various density matrix elements, which are uniformly consistent with those of the single-particle matrix elements of the E2 operator, and from the fact that significant strength is distributed to almost all elements in each transition. Angular momentum restrictions limit the possible particle-hole matrix elements to three for the 4^+ excitations and predictions are more varied for these transitions.

The shapes of the form factors calculated from these one-body-density matrix elements have been compared to amalgams of data from several sources[3-7] which span the region of momentum transfer 0.5 to 2.5 fm^{-1}. Except for ^{32}S, the predicted 2^+ form factors agree well with experiment out to abou 1.5 fm^{-1}. At larger values the theoretical magnitudes increasingly exceed the experimental values. In the context of the present model, the ^{32}S data seem to require a considerable larger transition radius than would be suggested by the values of the ground state rms radius. The predicted 4^+ form factors for strong states in ^{20}Ne, ^{24}Mg and ^{28}Si agree qualitatively with experiment but are also too large at larger momentum transfer.

The calculated form factors were normalized to the experimental data by choosing orbit-independent normalizations (equivalent to the squares of conventional isoscalar effective charges) which matched the predicted and observed maximum values. These normalization factors are in excellent agreement with effective charge values extracted from Coulomb excitation data for 2^+ states with these same wave functions. The existing data on strong 4^+ states suggests a rather stable E4 effective charge of approximately the same magnitude as the E2 effective charge.

Table 1. The matrix elements $\langle 4^+ \| (a^\dagger_j \otimes a_{j'})_{\Delta T=2,\Delta T=0} \| 2^+ \rangle (5)^{-1/2}$

Transition	(E_{x} - Mev)	5-5	5-1	1-5	5-3	3-5	1-3	3-1	3-3
									$= 2j-2j'$
^{20}Ne, 0→2	(1.75)	-0.407	-0.409	-0.356	-0.096	0.107	-0.164	0.218	-0.114
^{24}Mg 0→2	(1.56)	0.593	0.335	0.418	0.296	-0.290	0.162	-0.164	0.082
^{28}Si 0→2	(2.19)	0.313	0.404	0.585	0.308	-0.374	0.091	-0.157	0.196
^{32}S 0→2	(2.40)	-0.148	-0.258	-0.222	-0.256	0.230	-0.554	0.343	-0.157
^{36}Ar 0→2	(2.23)	0.140	0.174	0.158	0.147	-0.101	0.335	-0.240	0.555
^{20}Ne 0→4	(4.13)	0.403			0.271	-0.306			
^{24}Mg 0→4	(4.42)	-0.306			-0.008	-0.043			
^{24}Mg 0→4	(5.89)	0.240			0.308	-0.485			
^{28}Si 0→4	(5.29)	0.001			0.248	-0.486			
^{28}Si 0→4	(7.90)	-0.204			-0.157	0.489			
^{32}S 0→4	(4.82)	0.091			0.565	-0.333			
^{32}S 0→4	(6.65)	-0.092			-0.330	0.142			
^{36}Ar 0→4	(4.74)	0.125			0.460	-0.321			

FOURTH HIGH ENERGY HEAVY ION SUMMER STUDY, Berkeley, CA, July 24-28, 1978

INTERMEDIATE ENERGY HEAVY IONS -- FROM THE LOW ENERGY PERSPECTIVE

C. Konrad Gelbke

Let me first acknowledge all the people who either collaborated on the various experiments I would like to discuss or who made available their data prior to publication (Fig. 11.1). I have to apologize to everybody whom I did not mention and I'm pretty sure I forgot some of the people who gave me their data prior to publication or after publication.

As I was coming to Berkeley by airplane I remembered that two years ago at the summer study we talked a lot about flowers and weeds. Looking out of the airplane I tried to see some flowers on the ground, but I couldn't see any (Fig. 11.2). I wondered why. Finally when I walked up the hill this morning I took the path by foot and looked at all the stones and once in a while I saw a flower. So today I will take a rather pedestrian-type approach. I will remind you of all our everyday hardships and all the small niceties that we have encountered in low energy physics. I'm pretty sure that you know most of the facts, but as David Scott said, physicists like to hear what they already know, so I'll follow the tradition.

In order to organize my talk I'll follow the convention that one breaks up the reaction cross section into central collisions and into peripheral collisions (Fig. 11.3). At low energies, peripheral collisions are defined as elastic scattering, quasi-elastic scattering, and deeply-inelastic scattering (the latter class of reactions being a very interesting field of research in the last few years). At relativistic energies we talk about peripheral fragmentation reactions. At low energy, central collisions are generally fusion type reactions (at least for projectiles which are lighter than, let's say, mass 50), i.e., compound nucleus formation and some subsequent particle evaporation reactions or, for heavier target nuclei, de-excitation by fission. At relativistic energies a completely different picture has emerged. Here we are talking about nuclear fireballs, shock waves, pion condensates, and density isomers. You see I put two question marks to the right and to the left hand side of Fig. 11.3 because I'm pretty sure that this is not going to be the final word.

Now let me start very gently — with the most gentle process we know for heavy ion scattering, that is, the elastic process. Let me just remind you of what we have learned in the last few years about heavy ion elastic scattering (Fig. 11.4). (And actually it's not very much.) We know that we are only sensitive to the extreme tail region of the nuclear potential. The region where we can determine the optical potential reasonably well corresponds to a density overlap of the two nuclei of less than 10%. So if one plots a typical potential that is used in optical model calculations all the hatched region (marked by the question mark in Fig. 11.4) is not determined experimentally and hence is unknown. There is some evidence that we are getting more sensitive to slightly smaller radii if we increase the beam energy. There has been a very nice systematic study by Cramer and collaborators of the elastic

PROCEEDINGS OF THE INTERNATIONAL CONFERENCE ON NUCLEAR INTERACTIONS
Canberra, Australia, August 28-September 1, 1978

PION PRODUCTION NEAR THRESHOLD IN HEAVY ION COLLISIONS*

G.M. Crawley, W. Benenson, G. Bertsch, E. Kashy, and J.A. Nolen, Jr.

Cyclotron Laboratory, Michigan State University, East Lansing, MI 48824

and

J.O. Rasmussen, H. Bowman, M. Sasao, J. Ioannou, M.C. Lemaire+, J. Sullivan, and L. Oliveira

Lawrence Berkeley Laboratory, University of California

and

M. Koike and J. Chiba

University of Tokyo

The production of pions in heavy ion collisions near threshold is an extremely interesting problem both theoretically and experimentally. According to current theoretical ideas on pion-nucleon interactions, nuclear matter is not far from a phase transition involving the pion field. Models for the behavior of the pion in nuclear matter show peculiarities such as a near-zero or negative effective mass for the pion.[1] Under such conditions, pions can be produced in the interactions of nucleons with the potential field,[2] in addition to production in the collisions of nucleons with each other. The rate of pion production is thus increased by the potential field mechanism, and a characteristic angular distribution is predicted for the pions.

On the experimental side, the information on the pion production cross section at energies near threshold, obtained using emulsions,[3] is conflicting. In one case a very high pion multiplicity per collision is reported,[3] but in the other cases[4,5] a much lower upper limit for pion production is given. A theoretical prediction has been made for this cross section, based on production by nucleon-nucleon collisions alone.[6]

In the present experiment, measurements were made with 400 MeV/A and 250 MeV/A Argon beams from the Berkeley Bevelac incident on KCl and Pb targets. Pions were detected near 0° using plastic scintillator telescopes in a 180° magnetic spectrograph set up specifically for these measurements. A preliminary analysis of the data from the first run shows that the π^+ yield at 250 MeV/A is about a factor of three lower than at 400 MeV/A for the KCl target. The present data are consistent with the lower limit established by Lindstrom et al.[4] and Kullberg et al.[5] and disagree with the earlier measurements.[3] A comparison of the results with theoretical predictions will be presented.

*This material is based upon work supported by the National Science Foundation under Grant No. Phy 78-01684 and the Department of Energy.

+On leave from C.E.N., Saclay.

[1] Bertsch, G., and N. Johnson, 1975. Phys. Rev. D12:2230.

[2] Sawyer, R., 1976. Nucl. Phys. A271:235.

[3] McNulty, P.J., et al., 1977. Phys. Rev. Letters 38:1519.

[4] Lindstrom, P., et al., 1978. Phys. Rev. Letters, 40:93.

[5] Kullberg, R., et al., 1978. Phys. Rev. Letters 40:289.

[6] Malbrough, D., et al., Los Alamos preprint LA-UR-77-1939.

EIGHTH INTERNATIONAL CONFERENCE ON CYCLOTRONS AND THEIR APPLICATIONS
Bloomington, IN, September 18-21, 1978
IEEE Transactions on Nuclear Science, Vol. NS-26, No. 2, April 1979

THE MICHIGAN STATE UNIVERSITY SUPERCONDUCTING CYCLOTRON PROGRAM*

H. G. Blosser

Cyclotron Laboratory, Michigan State University
East Lansing, Michigan 48824

Summary

Status of the superconducting cyclotron program is reviewed as of September 1978. A number of design details have changed since the previous conference. Novel features have been checked in a variety of prototype test facilities.

Text

In June 1975 the MSU Cyclotron Laboratory received authorization to proceed with construction of a full scale prototype magnet for a 500 MeV superconducting cyclotron. The objective of this program was to establish basic feasibility of accelerator systems using such magnets. In May 1977 operating tests of the protoptype magnet were started; first operation at full design current occurred on May 26, 1977. Overall performance of the prototype magnet was excellent and in August 1977 the laboratory received authorization to proceed with a so called "Phase I" accelerator program, namely, a program to make the 500 MeV magnet into a working cyclotron and to connect this cyclotron with existing experimental facilities. This Phase I program is very much in mid-stream at present. First operating tests of the cyclotron are expected in the Fall of 1979 and nuclear physics use is expected to begin early in 1980. The laboratory has also submitted a proposal for a further major expansion, namely adding a second 800 MeV superconducting cyclotron as a booster for the 500 MeV machine and including additions to the laboratory building and to experimental facilities which would approximately double the size of the present installation. The proposal has received a high priority recommendation for funding in fiscal year 1980. If this proceeds as planned the full two cyclotron system is expected to come into use in early 1984.

Many of the subsystems of this overall project are described in specific topical papers appearing elsewhere in these proceedings i.e., central region, rf system, cryogenic system, magnetic field studies, trimming optimization studies, extraction studies, injection studies for the second stage, and overall design of the K800 cyclotron. The objective of this summary paper is to convey a somewhat more casual and largely pictorial glimpse of the actual status of the project as of September, 1978.

The core of the presentation is in the following six pages which present Figures 1 through 23. These figures and the technical comments included with the captions show a number of construction details of the K500 cyclotron and performance expected from the system. The figures also show a number of prototype assemblies built to test various features of the design.

In reviewing the figures, a number of major design changes can be seen relative to descriptions given at the 1975 cyclotron conference reflecting evolution of design concepts as the program evolved as well as adaptations to unexpected results from some protopype tests. The idea of using an inert superconducting extraction channel has been laid aside, for example, following a series of prototype tests of these so called "super-tubes", which gave a mixture of good and bad results and a sense of inadequate reliability of such elements as a key subsystem of a major accelerator project. The presently envisaged extraction system then consists of electrostatic deflectors which operate well within established technical limits on electric fields. The electrostatic deflectors are supplemented by sets of inert iron focusing bars positioned in a pattern which gives a field combining a strong quadrupole and a weak dipole component. The overall combination of deflector and focusing bars gives a very attractive extraction trajectory with excellent optical characteristics.

A major change in the rf system relative to the 1975 design is a lowering of the frequency range by an approximate factor of 3 and a correlated decision to make extensive use of harmonic numbers 1, 2, 4, etc., which require phasing of the dees by multiples of 120°. Phasing of 120° is a feature not previously used in cyclotrons except for a brief early test at Berkeley and a rather realistic model was therefore built to check tuning characteristics of a system of this kind. Orbit properties of the overall system are much improved by having the rf frequency more nearly match the orbital frequency and an overall sizeable improvement in beam quality is expected from the lower frequency system.

The lower frequency range involves dee stems of rather awkward length--at 9 Mhz the sliding short is $\sim$ 16' from the median plane--estimates of mechanical vibrations in dee stems of this length indicated serious problems for 4" diameter unsupported stems. Dee stem insulators have therefore been introduced just below the magnet yoke. These also then form a boundary for the vacuum envelope and allow the sliding shorts which tune the dees to operate in air.

The vacuum system for the cyclotron is a somewhat complicated three part chamber, namely a completely separate all metal enclosure as the insulating jacket for the main coil, secondly, a high quality cryopumped metal gasketed chamber for the beam space and thirdly, a low quality "coil" vacuum contained between the pole caps and the copper rf liners enclosing both pole tips and pole tip correction windings.

*Work supported by the U.S. National Science Foundation Grant #s 75-01080, PHY76-83254, and PHY78-01684.

EIGHTH INTERNATIONAL CONFERENCE ON CYCLOTRONS AND THEIR APPLICATIONS
Bloomington, IN, September 18-21, 1978

DESIGN CHARACTERISTICS OF THE K=800 SUPERCONDUCTING CYCLOTRON AT M.S.U.*

F. Resmini, G. Bellomo, E. Fabrici, H.G. Blosser, and D. Johnson
Cyclotron Laboratory, Michigan State University
East Lansing, Michigan 48824

Introduction

Design work on the proposed K=800, K_p=400, superconducting cyclotron at MSU has progressed to the point where overall machine characteristics are firmly established. The main purpose[1] of the machine is to serve as a booster for the K=500 cyclotron, now under construction. In this respect, let us recall that the design goal is to achieve maximum beam energies of 200 MeV/n for fully stripped light ions, and typically 30-40 MeV/n for heavy ions like uranium. Energy variability down to about 50 MeV/n and 4-5 MeV/n, again for light and heavy ions respectively, is also required to ensure some overlap with beam energies delivered by the K=500 in stand-alone mode.

Such an extreme range of beam energies, from very relativistic to non relativistic ones, demands a careful analysis of the intrinsic physics of the machine. Coupling to the first cyclotron, with the associated problems of beam injection and definition of the operating modes of both cyclotrons, is also a complex topic, and has indeed a number of consequences on the machine characteristics.

At this stage we believe that all major topics have been explored in sufficient detail so as to produce a consistent design. In the process, some unexpected findings led us to introduce a few unusual features, and it is the purpose of this paper to discuss the rationale behind them. For the sake of clarity, however, we shall first review the overall design as it stands now, turning thereafter to a detailed analysis of the single issues.

Outline of the Machine Design

A summary of the main cyclotron parameters is given in Table I, while a schematic horizontal layout and a vertical section are presented in Figs. 1 and 2. Choice of the pole radius, minimum hill gap, and sector spiral constant was mainly determined by the axial focussing requirements for 200 MeV/n fully stripped ions. A careful analysis of a number of different configurations indicated that the 41" pole radius was the minimum possible, and it has indeed been associated with a tight spiral and a hill gap of 2.5". In fact, a gap of 3" would already require, for the same spiral, a pole radius of 44"-45" at least. Average field B(r), ν_z and phase are presented as a function of radius in Fig. 3 for two examples of 200 MeV/n and 20 MeV/n beams, showing that the present configuration meets all acceleration requirements.

Table I. Main K=800 parameters.

Pole radius = 41"
Outer hill radius = 42"
No. of sectors = 3, 46° wide
Spiral constant = 1/13 rad/inch
Minimum hill gap = 2.5"
Maximum valley gap = 18"
Minimum-maximum operating fields = 30-50 kG
Yoke height = 117"
Yoke inner and outer diameters = 118"-174"
Total iron weight (poles included) ≃ 260 tons
R.F. frequency range = 9-32 MHz
Harmonic operating modes = 1st, 2nd
Peak dee voltage = 200 kV
R.F. power per dee < 150 kW
No. of trim coils = 22
Maximum total trim coil power ≃ 60 kW

Two peculiar features of the sector geometry are apparent from Fig. 1:

a. A counterclockwise-clockwise behaviour of the spiral, with a transition radius at about 15", which is required for stripping the injected particles in a hill. A detailed discussion of this aspect of the design is given in Ref. 2.

b. A radial cut of the profile from a radius of 40.8" to 42". This, as discussed in detail below, is needed to reduce ν_z values in the extraction region, thus avoiding a dangerous intrinsic resonance.

A central hole of 7" diameter is provided for insertion of the stripping foil position mechanism. Dee stems are inserted through 13" diameter holes at a radius of 31". Preliminary R.F. engineering studies indicate that, for the required 9 to 32 MHz range, the short circuit will have to move between 60" and 240" from the median plane, and therefore outside the yoke. It is anticipated that in this region the outer coaxial will be 18" diameter, and the inner one 8" diameter. The power figure quoted in Table I should be regarded at this stage as an upper limit.

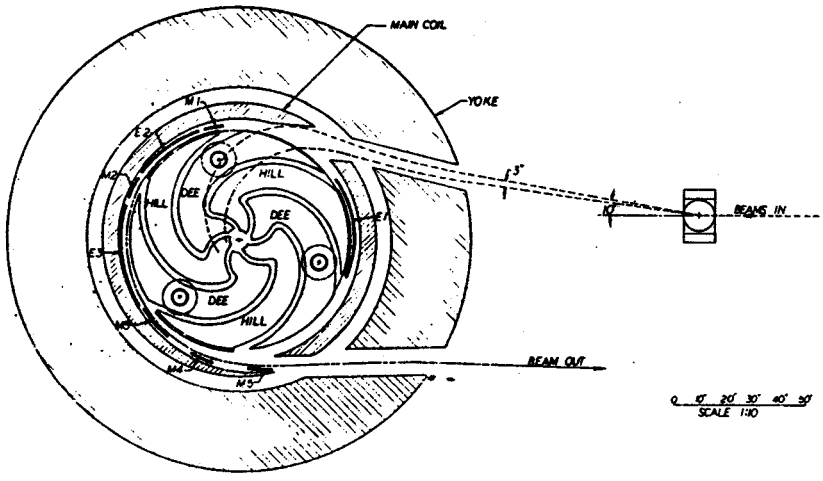

Fig. 1. Schematic layout of the K=800.

*This material is based upon work supported by the National Science Foundation under Grant No. Phy 78-01684.

0018-9499/79/0400-2078$00.75©1979 IEEE

EIGHTH INTERNATIONAL CONFERENCE ON CYCLOTRONS AND THEIR APPLICATIONS
Bloomington, IN, September 18-21, 1978

INJECTION STUDIES FOR THE K=800 SUPERCONDUCTING CYCLOTRON AT M.S.U.

G. Bellomo, E. Fabrici, and F. Resmini
Cyclotron Laboratory, Michigan State University, East Lansing, Michigan 48823

Introduction

Beam injection from the K=500 superconducting cyclotron, now under construction at MSU, into the proposed K=800 cyclotron obviously plays a major role in the successful coupling of the two cyclotrons. Let us recall that anticipated maximum beam energies[1] are between 200 MeV/n and 50 MeV/n for fully stripped light ions and heavy ions (uranium) respectively. Minimum energies for the same extreme cases are 50 MeV/n and 5 MeV/n. Operating center field values are between 30 kG and 47 kG, and Z/A values of accelerated particles range from 0.1 to 0.5. Focusing and bending requirements lead to a 41" pole radius machine, and a three sector geometry, having 46° wide hills, with an unusually tight spiral, i.e. with a constant of 1/13 rad/inch.

Although schemes of beam injection into superconducting cyclotrons have been studied before,[2,3] they were not addressed to machines with such a wide range of beam energies and extreme sector spiral. Furthermore, they concerned injection from electrostatic accelerators, while, as will be seen in the following, coupling between two cyclotrons imposes additional constraints on the injection scheme.

Therefore, an extensive study of the injection process was carried out. This led us to consider a rather new pole tip geometry as an alternative to a conventional spiral, in order to meet all injection requirements. It is the purpose of this paper to discuss in some detail the relative merits of the two solutions presently available.

Outline of Injection Requirements and Constraints

The main requirements are:

a. If at all possible, stripping should take place in a hill, to avoid having the stripping foil positioning and replacement mechanism inside a dee.

b. Injection trajectories should have an almost constant azimuthal entry position into the cyclotron, i.e. spanning 20-40 degrees at most.

c. As a consequence of (b), all trajectories could then originate from a fixed point outside the cyclotron. If the distance of this point is conveniently chosen, typically two to three times the cyclotron radius, then steering of just a few degrees at this point will assure for every beam the proper azimuthal entry position into the cyclotron.

d. Proper phase space matching to the cyclotron acceptance, both in the radial and axial spaces, should be possible.

Let us briefly review those aspects of the coupling of the two cyclotrons which pose intrinsic constraints on beam injection. We define: h, Z, Bo, Rex, and T/A as the harmonic number, charge state, center field value, extraction radius, and extraction energy of the first cyclotron (K=500) or second cyclotron (K=800), according to the subscript.

The basic requirement in the coupling of the two cyclotrons is that the R.F. acceleration frequencies in the two machines be the same. This hypothesis leads to the following consequences:

The second cyclotron acts just as an energy multiplier, so that in a non-relativistic approximation it must be:

$$\frac{T_2}{A} / \frac{T_1}{A} \simeq \left(\frac{Rex_2 \cdot h_1}{Rex_1 \cdot h_2}\right)^2 \qquad (1)$$

Thus, for any given final energy per nucleon, the injection energy depends solely upon the harmonic coupling ratio (HCR).

- The stripping radius R_S in the K=800, corresponding to the injection energy T_1/A, can be expressed as

$$R_S = Rex_1 \frac{h_2}{h_1} \qquad (2)$$

and therefore, for a given Rex_1 (in our case 26.4"), it is constant for any given HCR and does not depend upon charge state or energy of the ion.

- The stripping ratio Z_2/Z_1 must obey the relationship

$$Z_2/Z_1 = \frac{h_1 Bo_1}{h_2 Bo_2} \qquad (3)$$

On the other hand, from the hard edge approximation, a limit can be derived for the lower limit of the admissible stripping ratio for injection, i.e.:

$$Z_2/Z_1 \geq \frac{1}{2}\left(\frac{Rex_2 \, h_1}{Rex_1 \, h_2} + 1\right) \qquad (4)$$

In our case, since $\frac{Rex_2}{Rex_1} \simeq 1.5$, one obtains, for typical HCR of 3:1, 4:1, and 5:1, lower limits of $Z_2/Z_1 = 2.8, 3.6, 4.4$, respectively. Although the hard edge approximation is not really verified in a realistic cyclotron, the limits given by the above formula represent very reasonable guidelines.

Careful analysis of the operating range of the K=800 cyclotron has determined[1] that only the following harmonic coupling ratios are possible:

- 3:1, 4:1, 5:1 for beam energies between 200 MeV/n and 18 MeV/n, the lower limit being imposed by the R.F. frequency. Corresponding average stripping radii are 8.8", 6.6", and 5.2".
- 5:2 and 7:2 for energies between 5 MeV/n and 60 MeV/n, in this case the upper limit being determined again by the R.F. frequency. Corresponding stripping radii are 10.5" and 7.5".

In view of the above constraints, the self-consistent analysis of beam injection involves the following steps:

- Determine the ranges of stripping ratios needed for each harmonic coupling, over the whole $(Bo_2, Z_2/A)$ operating range. These must satisfy the relationships (2), (3), and (4) and the Z_2 values must also, for each energy, be at,or around,the peak for maximum intensity at stripping.[1]
- Determine an injection scheme which fulfills requirements (a), (b), and (c) set forth above.
- Determine the real lower and upper limits of the stripping ratio Z_2/Z_1 which are compatible with the selected injection scheme. This must be done for each of the five possible harmonic couplings over the entire range of Bo_2, Z_2/A.
- Verify that the Z_2/Z_1 limits thus derived allow the desired coupling of the two cyclotrons.

0018-9499/79/0400-2090$00.75©1979 IEEE

EIGHTH INTERNATIONAL CONFERENCE ON CYCLOTRONS AND THEIR APPLICATIONS
Bloomington, IN September 18-21, 1978

A METHOD FOR MINIMIZING TRIM COIL POWER REQUIREMENTS IN SUPERCONDUCTING CYCLOTRONS*

G. Bellomo and F. Resmini
Cyclotron Laboratory, Michigan State University, East Lansing, Michigan 48823

Introduction

A key issue in the design of superconducting cyclotrons is to obtain a properly isochronous field over the wide range of particles and energies usually demanded. In this respect it is useful to recall that in superconducting cyclotrons the main coils produce a large fraction of the total average field, and that the field produced by the saturated iron is very nearly constant over the 20-50 kG range usually employed.

The main problem is therefore to optimize the main coil design, and to optimize the field generated by the iron, in order to minimize the total power requirements for trim coils. Detailed studies for the proposed K=800 machine at MSU, which requires isochronous fields for ion energies spanning from 5 to 200 MeV/n, led us to develop a method which effectively helps in solving the problem. In the process, we found some results which seem to have an overall validity and therefore have some implications for superconducting cyclotron design. It is the purpose of this paper to review in some detail the procedure used and the main consequences pertaining to the K=800 design study.

Outline of the Method

We assume the main coils to be split into two vertical sections, subscript α referring to the lower section (closer to the median plane) and subscript β to the upper one. The following notation will be used throughout:

- $F_\alpha(r)$, $F_\beta(r)$, $F_k(r)$ = form factors of the main coil sections and of the kth trim coil (with resistance R_k, N coils total).
- I_α, I_β, I_k = corresponding currents
- $B_{iron}(r)$, $B_{is}(r)$ = magnetic field generated by the iron configuration and isochronous field required by a given ion
- $\epsilon(r)$ = field error, with respect to isochronism.

We shall then write, for any ion:

$$B_{is}(r) = B_{iron}(r) + F_\alpha(r)I_\alpha + F_\beta(r)I_\beta + \sum_{K=1}^{N} F_k(r)I_k + \epsilon(r) \qquad (1)$$

It is obvious that given $B_{iron}(r)$, $F_\alpha(r)$, $F_\beta(r)$, and $F_k(r)$, ordinary least squares fitting will yield the I_α, I_β, and I_k values which minimize $\sum_r \epsilon^2(r)$.

It is also obvious that for any particular ion, and whatever the functions $F_\alpha(r)$ and $F_\beta(r)$ are, there will always be a function $B_{iron}(r)$ for which the currents I_k and the errors $\epsilon(r)$ in that particular case equal zero.

The problem to which we address ourselves can instead be schematized as follows:

- Given a main coil, i.e. $F_\alpha(r)$ and $F_\beta(r)$, and trim coil form factors $F_k(r)$, determine, if it exists, a $B_{iron}(r)$ which minimizes:
  $\sum \epsilon^2(r)$ and $P = \sum_{K=1}^{N} R_k I_k^2$ (total trim coil power)
  over the desired range of ions and energies.

As a consequence, optimize the main coil design, with the aim to minimize the total trim coil power.

Our method is based upon the selection of two appropriate particles which, for the present purpose, can be thought of as representative of the extreme isochronous fields required, like the least and most relativistic particles in the operating range of the cyclotron.

If we write eq. (1) for these two ions, represented by subscripts 1 and 2 on the relevant quantities, and then subtract the two equations, we get:

$$[B_{1is}(r)-B_{2is}(r)] = [B_{1iron}(r)-B_{2iron}(r)] + F_\alpha(r)[I_{1\alpha}-I_{2\alpha}] + F_\beta(r)[I_{1\beta}-I_{2\beta}] + \sum_{K=1}^{N} F_k(r)[I_{1k}-I_{2k}] + [\epsilon_1(r)-\epsilon_2(r)] \qquad (2)$$

with self-explanatory notation.

Let us now make the simplifying hypothesis:

$$B_{1iron}(r) - B_{2iron}(r) \equiv 0 \qquad (3)$$

for every radius.

This physically corresponds to an invariable field produced by the saturated iron configuration. Although not exactly fulfilled in reality, it nevertheless is an accurate enough hypothesis for the present purposes. We shall anyhow examine later the consequences of it not being strictly verified.

Equation (2) can then be written as

$$\Delta B_{is}(r) = F_\alpha(r)\Delta I_\alpha + F_\beta(r)\Delta I_\beta + \sum_{K=1}^{N} F_k(r)\Delta I_k + \Delta\epsilon(r) \qquad (4)$$

where the symbol Δ represents the differences in eq. (2).

Having eliminated $B_{iron}(r)$, equation (4) lends itself to a minimization, with an ordinary least squares fitting procedure, of the quantity: $\sum_r [\Delta\epsilon(r)]^2$, thus obtaining values of:

$$\Delta I_\alpha = I_{1\alpha} - I_{2\alpha} \qquad (4a)$$
$$\Delta I_\beta = I_{1\beta} - I_{2\beta}$$
$$\Delta I_k = I_{1k} - I_{2k}$$

One can prove[1] that if $\sum_r [\Delta\epsilon(r)]^2$ is minimized with a least squares fitting, then also

$$\sum_r \epsilon_1(r)^2 + \sum_r \epsilon_2(r)^2 \quad \text{and} \quad P_1 + P_2$$

will be minimized, if

- $\epsilon_1(r) + \epsilon_2(r) = 0$ for every radius (5)
- $I_{1k} + I_{2k} = 0$ for every trim coil

This finding has the following consequences:

- Given two ions, and for given main coils and trim coils, there exists an absolute minimum of the trim coil power needed for providing an isochronous field in the two cases. This minimum value is obtained by least squares fitting of eq. (4), imposing thereafter condition (5). This power is thus equal for both ions, and corresponds to equal and opposite currents for each trim coil.
- To reach the condition of absolute minimum power the pole tips must produce a $B_{iron}(r)$ which satisfies for every radius the following equation:

*This material is based upon work supported by the National Science Foundation under Grant No. Phy 78-01684.

0018-9499/79/0400-2095$00.75©1979 IEEE

EIGHTH INTERNATIONAL CONFERENCE ON CYCLOTRONS AND THEIR APPLICATIONS
Bloomington, IN, September 18-21, 1978

BEAM EXTRACTION SYSTEM FOR THE K=500 SUPERCONDUCTING CYCLOTRON

M.M. Gordon and E.M. Fabrici
Cyclotron Laboratory, Michigan State University, East Lansing, Michigan 48824

Abstract

In addition to three electrostatic deflectors, the proposed extraction system contains six sets of "focusing bars." Calculations are presented to demonstrate the usefulness of these elements for both beam deflection and focusing. Next, the troublesome field perturbations produced by the focusing bars are discussed, together with the design for "compensating bars." Pre-extraction orbit calculations are then presented to show the evolution of the radial and axial phase space areas associated with the accelerating beam, and to demonstrate the effects of various resonances including those generated by the focusing bars.

1. Introduction

The general features of the K=500 Superconducting[1] cyclotron are described elsewhere in these proceedings. This cyclotron will utilize the "precessional" extraction method which has proven so successful in our present machine and in many other isochronous cyclotrons. The basic procedure consists in accelerating the ions out beyond the isochronous region into the edge region of the magnetic field, thereby passing through the $\nu_r=1$ resonance where the addition of a carefully controlled first harmonic "field bump" drives the orbits off center. The resultant orbit precession then produces the necessary large radius gain per turn at the entrance of the electrostatic deflector.

Before discussing the pre-extraction orbit calculations in detail, we first consider the hardware required to deflect the beam out of the cyclotron. Fig. 1 shows a schematic diagram of this hardware according to the present design. In order to complete beam deflection in less than one turn, we require three electrostatic deflectors together with a series of six short magnetic channels, called "focusing bars". For simplicity, the three electrostatic deflectors will be fixed in position and have fixed apertures. Our orbit calculations indicate that electric fields less than 110 kV/cm should suffice in all cases, and considering the "VE law" together with our own experience, we feel confident that an aperture as large as 10 mm can be used without serious sparking problems.

2. Focusing Bars

Focusing bars are extremely useful for beam extraction since they provide a fairly strong focusing gradient together with a deflecting field which can be varied significantly. One set of these bars consists of three rectangular steel rods which enclose the beam as shown in Fig. 2. When situated in the strong field of the cyclotron, these bars become magnetized to saturation, and generate a quadrupole-like field within the aperture occupied by the beam.

The magnetic field produced by the focusing bars can be calculated quite easily by assuming they are uniformly magnetized in the vertical direction. The validity of this assumption has been checked, at least in the two dimensional case, by use of the "TRIM" program which employs a sophisticated relaxation calculation. For a standard magnet steel with a 21.2 kG saturation field, the two calculation methods were found to agree very well for external field all the way down to about 5 kG. Below this level, the assumption of saturation becomes progressively poorer.

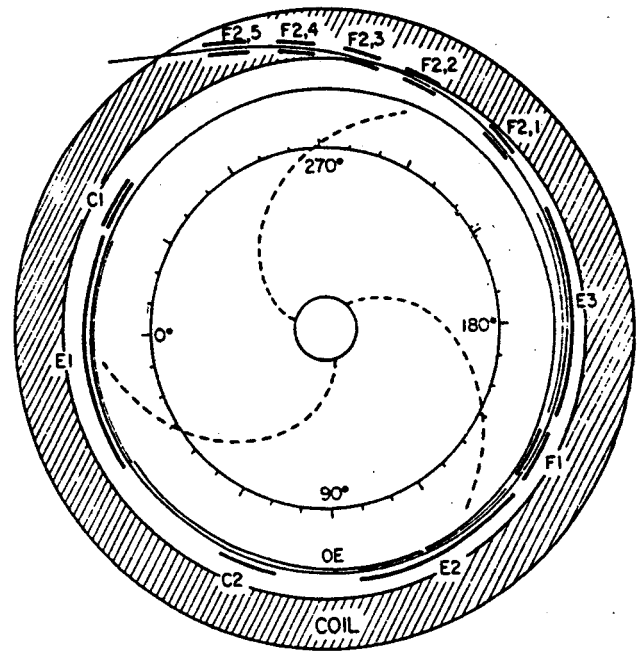

Fig. 1. Schematic Diagram of the Extraction System. The elements shown are three electrostatic deflectors (E1, E2, E3), six sets of focusing bars (F1, F2.1-F2.5), and two sets of compensating bars (C1, C2). All of the focusing bars have the same aperture a = 0.5 inch, corresponding to a focusing gradient of 9.6 kG/inch, and a field decrement of 0.9 kG at the center of the aperture. The elements C1 and C2 are designed to compensate for the first harmonic field components produced by the two groups of focusing bars, F1 and F2, respectively.
The curve labeled OE represents the envelope of all the internal orbits prior to extraction (see Fig. 5). The two large circles at r=30 and 36 inch indicate the boundaries of the superconducting coils. The three broken spiral curves locate the centers of the three magnet hills. Scale markings for the azimuthal angle θ are shown on a reference circle at r=20 inch.

Fig. 2 shows a plot of the median plane field and the corresponding field gradient as a function of x, the radial displacement from the center of the aperture. These results pertain to a set of focusing bars having the "standard" geometry: (height)/(width) = a/(a/4), where a is the aperture, and in our case, a = 0.5 inch. This cross sectional geometry is also shown in Fig. 2. The length of the bars here is l = 4.0 inch, and the plotted fields refer to a point halfway from each end.

The strong gradient of the focusing bars opposes the radially defocusing gradient associated with the edge region of the cyclotron field through which the extracted beam must pass. As shown in Fig. 2, the focusing gradient is not only strong, but is also nearly constant over about 80% of the aperture. In our case with a = 0.5 inch, this gradient has an average value of 9.6 kG/inch, and varies by only ± 0.6 kG/inch over an interval Δx = 0.4 inch.

0018-9499/79/0400-2101$00.75©1979 IEEE

EIGHTH INTERNATIONAL CONFERENCE ON CYCLOTRONS AND THEIR APPLICATIONS
Bloomington, IN, September 18-21, 1978

DESIGN OF THE CENTRAL REGIONS FOR THE MSU 500 MeV SUPERCONDUCTING CYCLOTRON*

E. Liukkonen,** J. Bishop, S. Motzny and T. Antaya
Cyclotron Laboratory, Michigan State University
East Lansing, Michigan 48824

Abstract

Different central regions for the MSU 500 MeV superconducting cyclotron are designed and extensively studied in order to find central regions which would yield desired beam qualities for the wide variety of ions and energies which we plan to accelerate. Coupled operation of the 500 and 800 MeV superconducting cyclotrons is included in this study.

1. Introduction

The requirements of a good central region for the MSU 500 MeV superconducting cyclotron are more stringent than those for a cyclotron using conventional magnets. A good beam quality is desirable for the large variety of particles and energies for which the 500 MeV superconducting cyclotron should operate, both as a stand-alone accelerator and as an injector to the 800 MeV superconducting cyclotron.

The high magnetic field strength of the superconducting magnet, which is about three times higher than in conventional cyclotrons, influences the design of the central region. Particles with high charge to mass ratios will bend very strongly during the first revolution, thus leaving only a very small free space for an ion source. As will be seen later, special attention has been required to overcome the clearance problems close to the ion source, especially in the first harmonic mode of acceleration.

Instead of the constant orbit geometry applied in the MSU 50 MeV cyclotron, the new 500 MeV cyclotron will make use of a fixed dee voltage (100 kV) and variable turn number, ranging from 45 to 535. Due to a 3-fold dee structure (3 dees and 3 dummy-dees) and 3-phase operation of rf voltage, the electric field is very complicated in the centre of the cyclotron where a strong electric focusing is needed. The dees are so "thin" in azimuth that there is practically no electric field free area in the first few turns. Therefore all orbit calculations in the central region have to be based on realistic electric fields. The 3-dimensional electrolytic tank measurements of electric fields have been an essential part of this study.

In the course of development, the frequency range of the 500 MeV cyclotron has changed considerably from the originally proposed range of 27-84 MHz, in which it was intended to operate in the 3rd and 9th harmonic modes of acceleration. Detailed studies of this frequency range revealed two relatively serious sources of difficulties, namely that the large physical size of the dees causes a severe voltage gradient to occur along the dees when operated at high frequencies, and transit-time problems between the ion source and puller were shown to exist on the higher harmonics. This second difficulty would force the use of a dc bias on the ion source, which is not desirable due to the expected maintenance problems. To overcome these problems a much lower frequency range was introduced, 9-32 MHz. This frequency range is excellent for coupled operation of the 500 and 800 MeV cyclotrons, but it will require 1st harmonic acceleration in the stand-alone use of the 500 MeV cyclotron for the most interesting high-energy light heavy ions.

The operational requirements for the central region are so extensive that it is obvious more than one central region is needed to fulfill all these conditions. On the other hand, one likes to keep the number of central regions as small as possible.

2. Electrolytic Tank Measurements of Electric Fields

The electric fields are measured using a full-scale 11 inch diameter electrolytic tank model of the center of the cyclotron. The three dees and three dummy dees are represented by copper plates set 1/2 inch below water surface to correspond to the one inch dee height. To simplify construction and data-taking, the mirror image of the electrode system relative to the median plane is omitted; placing the water surface at this plane imposes the proper boundary condition. A photo in Fig. 1 shows a model which is built for the first harmonic mode of operation.

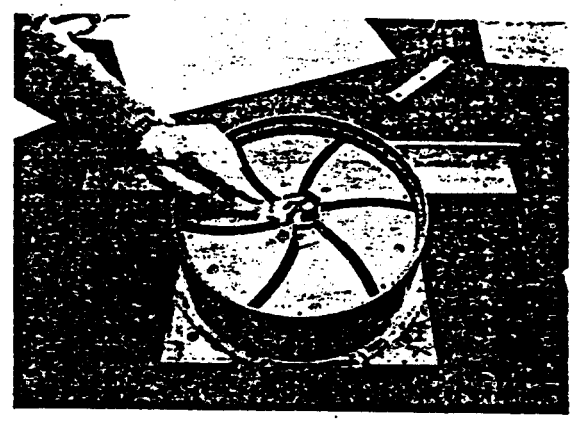

Fig. 1. Photograph of three dimensional electrolytic tank used to obtain central region electric field maps. The forefinger points to the extraction electrode (the "puller") on dee #1 and the cylinder near the puller represents the source. The top surface of the central electrodes corresponds to the median plane of the system. Electrodes in the tank are full size and the electrode system in the photo is set up for cyclotron operation on the first harmonic mode.

The gap between each dee and its neighboring dummy dee is 1/2 inch. In order to decrease field penetration on the first turn both the gap and the dee height are reduced, and the posts extend through the median plane. It takes about six hours for one complete measurement with a 140 by 140 mesh in 0.04 inch steps. The measurement system shows a very small r.m.s. of one part in one thousand from a check with a parallel geometry.

*This material is based upon work supported by the National Science Foundation under Grant No. PHY 78-01684.
**Supported by the Academy of Finland; permanent address: University of Jyvaskyla, Jyvaskyla, Finland.

0018-9499/79/0400-2107$00.75©1979 IEEE

EIGHTH INTERNATIONAL CONFERENCE ON CYCLOTRONS AND THEIR APPLICATIONS
Bloomington, IN, September 18-21, 1978

MAGNETIC FIELD MEASUREMENTS IN THE MSU 500 MEV SUPERCONDUCTING CYCLOTRON*

P. Miller, H. Blosser, D. Gossman, B. Jeltema, D. Johnson, P. Marchand
Cyclotron Laboratory, Michigan State University, East Lansing, Michigan 48824

Summary

The measurements of the magnetic field in the superconducting cyclotron under construction at Michigan State University are reported. The 55-channel flip coil gaussmeter built at MSU for this purpose is described. Twelve field maps measured with various currents in the two sections of the main coil have been Fourier-analyzed for evaluation of magnetic imperfections and data errors and for comparison with calculated magnetic field distributions. The calculation procedure is in excellent agreement with the measured data. The imperfection harmonics are small and there is evidence in the measurements that they are partly correctable by better alignment of pole tips and coil tank at final assembly of the cyclotron.

Apparatus

The gaussmeter uses 55 flip coil/integrator sets with computer controlled data scanning. The hardware is similar in concept to that developed to map the field of the Oak Ridge Cyclotron[1].

Moving parts are mostly non-metallic to reduce eddy current effects. The coils are wound on Delrin bobbins with an outer diameter of 3/8", and contain about 500 turns of #34 AWG enamelled copper wire (R=16Ω). They are mounted .5" apart in holes drilled in a 7/8" dia. rod made from G-10 epoxy-fiberglass material. The rod is rotated by strings connected to a non-magnetic air operated piston. The probe mechanism has to fit within the 1" magnet gap between pole liners. The azimuthal drive mechanism and the strings for rotation of the rod pass through the center hole in the magnetic yoke. Electrical wires are routed through another large hole in the yoke. The azimuthal scanning is done with a stepping motor coupled to a worm drive. The stepping motor requires a 3-layer cylindrical magnetic shield to keep it from stalling in the fringe field near the yoke at full magnet excitation. The entire apparatus works automatically under computer control through a complete field map.

The integrators consist of Analog Devices type 234L operational amplifiers with a feedback network time constant RC=0.022 sec. In the early design stages, temperature compensated ceramic capacitors seemed to be the best choice, and temperature regulation of the integrators was thought to be unnecessary. Further testing revealed that polystyrene capacitors, having negligible leakage and smaller dielectric polarization, would be a better choice in spite of their negative temperature coefficient of about 10^{-4}/°C. The effect of a temperature change on the coils and the integrators has been measured, as described below. Due to procurement difficulties, two different size capacitors had to be used to complete the full array of integrators.

Five integrators are assembled in one NIM module. Eleven modules are therefore required. A Hewlett Packard 3490 A digital voltmeter scans through the integrators by means of a reed relay multiplexer (Matrix Corp. 1701). The measurement cycle for 55 integrators takes about 18 sec (relay setting time 100 msec plus measurement time of 230 msec per channel). The voltmeter is inherently insensitive to noise pickup at the power line frequency or its harmonics. The calibration constant for each channel was obtained by operating the apparatus in a uniform field measured with an NMR probe. Calibrations at 4 fields (1.5 to 13.5 kilogauss) confirm the integral linearity of the response to within 0.03%. If extrapolated linearly to 60 kilogauss this would produce a calibration error $\leq$ 0.14%.

*This material is based upon work supported by the National Science Foundation under Grant No. Phy 78-01684.

The magnetic field $B=k\Delta V$ is inferred as the product of the coil-integrator calibration constant k and the average integrator voltage change for two flips (one up and one down). Thus, a linear integrator drift is cancelled. (Typical integrator drift rate is 0.1 mV/sec.; the time between measurements before and after a flip is about 20 sec.). To correct for temperature changes one would multiply k by the factor

$$(1 + C_E \Delta T_E - C_C \Delta T_C),$$

where the last two terms refer to the coils and the electronics, and the ΔT's represent temperature changes relative to the temperature at the time the calibration constant k was determined. Average values of the experimentally measured coefficients are given in Table 1.

Table 1. Typical Fluxmeter Properties

Type	Integrator Components	No. of units	C_C (C^{-1})	C_E (C^{-1})	avg. noise (T)	avg. k ±S.D. (T/V)
1	.022uf 1M	41	9×10^{-5}	3×10^{-4}	$.9\times10^{-4}$	.675±.020
2	.1 uf 220K	14	5×10^{-5}	8×10^{-5}	$.6\times10^{-4}$	.672±.021

The two types of integrator exhibit different average temperature coefficients. The coil temperature coefficients are found to lie between the thermal expansion predictions for the plastic coil form (2×10^{-4}) and the copper conductor (3×10^{-5}), as expected, since temperature induced variation of coil resistance is negligible. The temperature coefficient of the electronics operates with opposite sign from the anticipated one due to the capacitance change. We suspect that the temperature coefficient of the resistors is larger than expected, but this has not been verified.

Because the temperature fluctuations during mapping were small (≈1°C) the temperature corrections were not included in the computer program, although temperature data were recorded with the field maps automatically. The temperatures of the probe arm and three of the integrator modules are registered by four calibrated thermistors in series with a precision shunt and a d.c. power supply. The thermistor and shunt voltages are read by the computer every time the integrators are read.

Stability and Precision

A special computer program tests the repeatability and stability of the entire system. The computer repeatedly flips the measuring bar and stores the magnetic field measured by each integrator and the time on a file for later processing. The bar azimuth is not changed during the measurements. All 55 channels show a downward drift of the magnetic field of about 6 gauss in one hour, apparently the result of drift of the power supply current. This effect as well as any uniform temperature-induced drift is corrected during magnet mapping by normalizing the measurements to keep the central field constant.

The magnetic field history from each integrator is fitted to a second degree polynomial, since the drift rate is not uniform but can be seen to decrease with time in a plot of the data. The rms deviation of the

0018-9499/79/0400-2111$00.75©1979 IEEE

EIGHTH INTERNATIONAL CONFERENCE ON CYCLOTRONS AND THEIR APPLICATIONS
Bloomington, IN, September 18-21, 1978

OPERATING EXPERIENCE WITH THE MICHIGAN STATE UNIVERSITY SUPERCONDUCTING CYCLOTRON CRYOGENIC SYSTEM*

M.L. Mallory
Cyclotron Laboratory, Michigan State University
East Lansing, Michigan 48824

Abstract

The MSU superconducting cyclotron cryogenic system has been operating for about one year and many cryogenic parameters have been measured. Data for cryostat cooldown, liquid helium consumption, liquid nitrogen consumption, cryostat warmup, and vacuum jacket pressure as a function of temperature have been taken. In addition, methods have been developed for handling of contaminants in the helium system (air), for filling liquid helium in the cryostat, and for various cryogenic failure modes. Finally, a leak detection method was developed that is applicable at liquid helium temperature and has been used to find ultra-small leaks in the cryostat. This method utilizes the density and viscosity variations of cold helium gas as a function of temperature and may ultimately provide three orders of magnitude sensitivity improvement beyond presently achieved room temperature leak rates.

Introduction

A superconducting heavy ion cyclotron magnet[1] is now successfully operating at Michigan State University. The major effort at turning this magnet on and its subsequent operation has been predominately the task of understanding various cryogenic problems. The majority of these problems can be classified as understanding the practical knowledge of operating a cryogenic system, i.e., versus some fundamental or new aspects of cryogenics.

In acquiring the necessary knowledge to run the cryogenic system, the invaluable advice of various cryogenic experts has been obtained, but, as to be expected, problems have been encountered that were not considered. The characteristics of the Michigan State University cryogenic system and various operating experiences are reported in the following sections with the expectation that future superconducting cyclotrons will profit from these results.

Cryogenic System Characteristics

The cryogenic system of the superconducting cyclotron is a closed helium loop. The major components of the system are 1) the magnet cryostat, 2) a 9733 gallon helium gas reservoir tank, 3) a 500ℓ liquid helium dewar, 4) a CTI 1400 refrigerator-liquifier with dual charcoal filter traps at 60 K and variable engine speed control, 5) two 55 cu ft/min helium compressors, and 6) all interconnecting helium transfer lines. An existing liquid nitrogen system was used and required construction of transfer lines to the appropriate ports. Fig. 1 is a block diagram of the superconducting cyclotron helium system.

An important part of the system is the instrumentation used to monitor the cryogenic parameters. Shown in Fig. 2, it includes four platinum thermometers, twelve tophel-cupron thermocouple junctions, and eight helium level sensors. Various temperature and pressure gauges are included on the refrigerator.

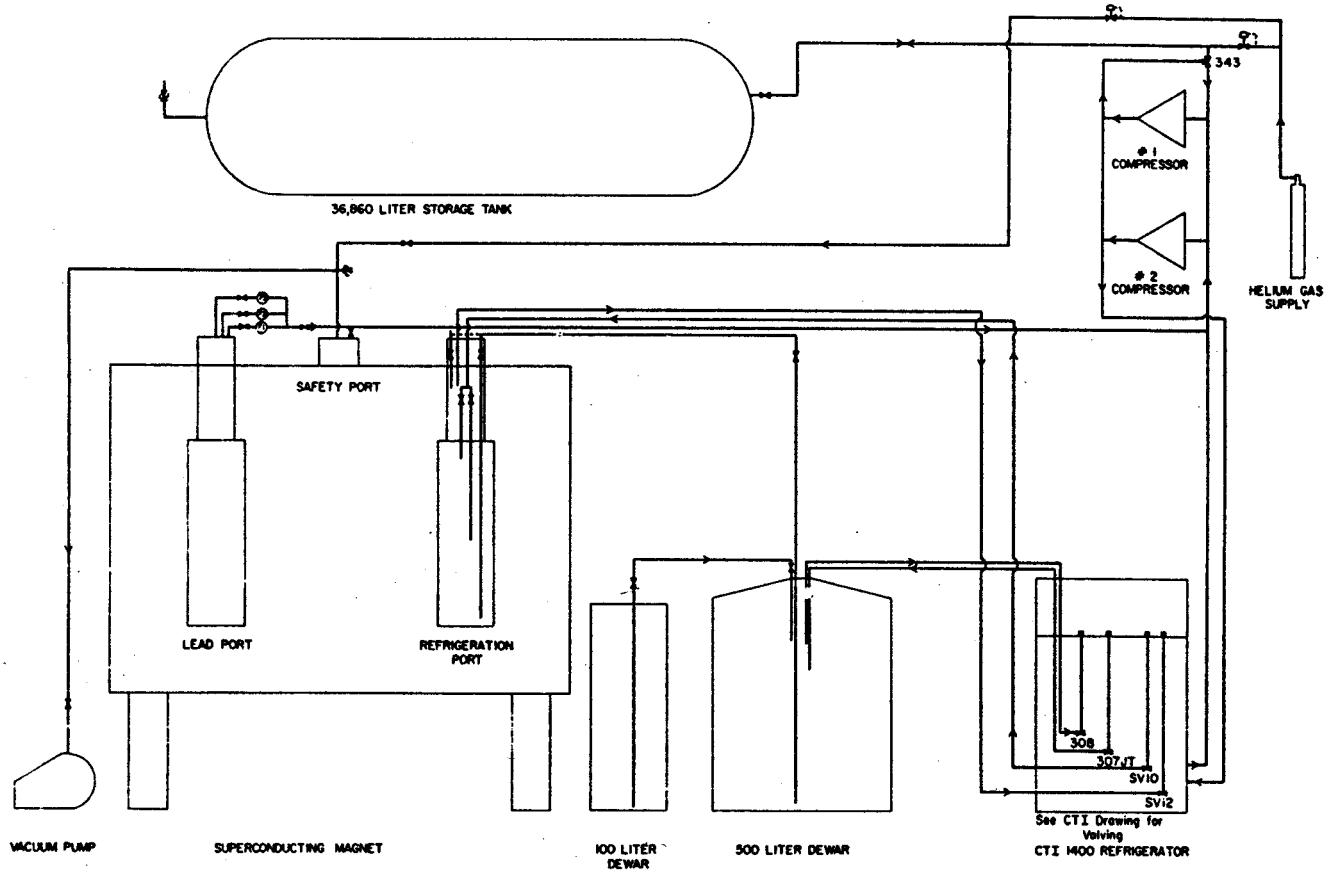

Fig. 1. The helium system block diagram for the 500 MeV superconducting cyclotron. The system is a closed helium loop and has a liquid helium production capacity of 26 ℓ/hr.

*This material is based upon work supported by the National Science Foundation under Grant No. Phy 78-01684.

EIGHTH INTERNATIONAL CONFERENCE ON CYCLOTRONS AND THEIR APPLICATIONS
Bloomington, IN, September 18-21, 1978

BEAM EMITTANCE MEASUREMENTS WITH A DISPERSION-MATCHED MAGNETIC SPECTROGRAPH *

P.S. Miller, E. Kashy and J.A. Nolen, Jr.
Cyclotron Laboratory, Michigan State University, East Lansing, Michigan 48824

Summary

The technique of dispersion-matching a beam to the split pole magnetic spectrograph at the MSU Cyclotron Laboratory was employed to eliminate the broadening of the beam spot size due to the coherent energy variations which come mainly from fluctuations of the amplitude of the cyclotron dee voltage. The incoherent emittance can therefore be measured directly.

This was accomplished by observing the spot size in the focal plane of the spectrograph with a high magnification television system and by measuring the beam divergence angle with a simple intercepting probe placed upstream. The emittance for proton beams was in agreement with previous indirect measurements. The luminosity of a proton beam was approximately equal to that inferred from previous d.c. test stand measurements. Measurements for $^{3}He^{2+}$ and $^{12}C^{4+}$ beams are also presented. The contribution to the divergence angle by the coherent energy spread was found to be negligible, in agreement with calculation. The correlation of observed line width with ion source slit width suggests that the complete optical system from ion source to the spectrograph is linear, and that an image of the ion source slit was observed in the spectograph focal plane.

Introduction

A television-scintillator beam detection system has been developed[1] for rapid tuning of the beam transport system to a "dispersion match" between the beam and the magnetic spectrograph. We adapted it to allow us to make direct measurements of the incoherent radial emittance of the accelerator beam. This quantity was inferred by Blosser[2] from standard emittance measurements on the dispersed beam by comparing them in detail with calculations giving the effect of dispersion on the beam distribution. The result for 40 MeV protons was 0.7 mm-mrad. A subsequent (unpublished) measurement with refined apparatus reduced the value to 0.3 mm-mrad. The present direct measurements have confirmed this more recent result. The method has also been applied to two other beams, 70 MeV $^{3}He^{2+}$ and 77 MeV $^{12}C^{4+}$.

Method

The direct beam was brought through the spectrograph to a focus on the scintillator in the focal plane. After passing through the scintillator it was stopped in a Faraday cup, which measures the beam current, as shown in Fig. 1. The beamline quadrupoles and the position of the plate holder, which supports the apparatus shown in the figure, were adjusted to give minimum line width, which is the condition for a focus and matched dispersion. The spot size Δx and the divergence angle $\Delta\theta$ were measured. The emittance area of the beam ellipse is $\pi/4\ \Delta x\ \Delta\theta$, where Δx and $\Delta\theta$ represent the full axis of the ellipse. The small wires in front of the scintillator were visible in the television picture. Their diameter and spacing served to calibrate the distance scale. An example of the television display, from which the line width was measured, is shown in Fig. 2. The full width of the beam spot was used. The precision is ±.005 mm for the high magnification used for the proton and He^{3} measurements.

The angular divergence of the beam was measured with a transversely movable probe located 22 inches upstream from the focal point in the camera box of the magnetic spectrograph. The probe consisted of a tantalum plate with an attached .030" dia. tungsten wire that was clamped at one end in a bracket attached to the plate. As the probe was moved across the beam the current from it was measured. The wire signal gave a direct measure of the beam profile, but was subject to broadening from imperfect wire alignment. The occultation of the beam by the edge of the plate gave a more reliable measure of the beam width. The positions where 10% and 90% of the beam was transmitted were taken to define the divergence angle (includes 80% of the beam). The precision is estimated to be ±.7 mrad, partly due to beam intensity fluctuations. Simultaneous strip chart records of the probe current and the beam current transmitted past the focal plane to the Faraday cup are shown in Fig. 3.

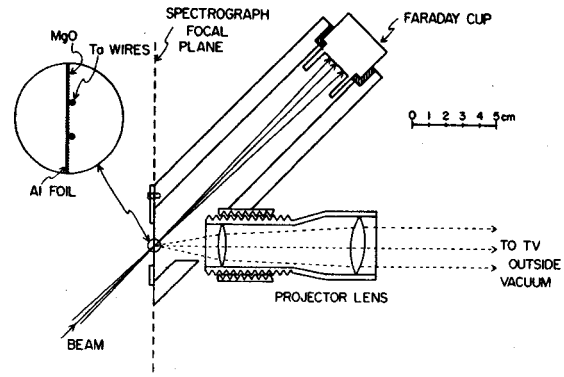

Fig. 1. Viewing apparatus positioned in the spectrograph focal plane. Light from the lens traverses a plastic window before entering the television camera lens. The two vertical wires in the insert, which are 25 μm in diameter and are separated by 2 mm, serve to calibrate the width and relative position of the beam image.

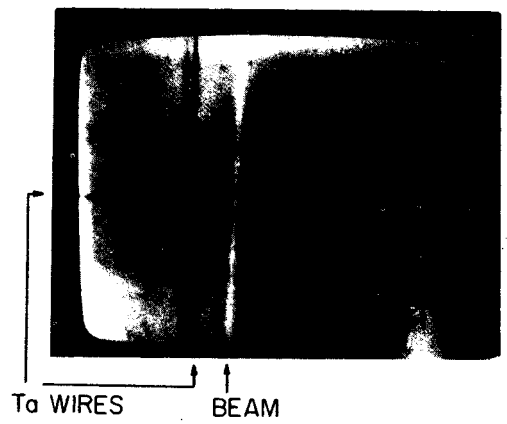

Fig. 2. Photograph of the television picture of the beam (white image) on the MgO scintillator. Only one of the two vertical wires is seen at this high magnification. Its shadow on the scintillator is also visible. The diameter of the wire is 25 μm. The tilt of the beam image is an indication of a small beam misalignment.

*This material is based upon work supported by the National Science Foundation under Grant No. Phy 78-01684.

0018-9499/79/0400-2334$00.75©1979 IEEE

EIGHTH INTERNATIONAL CONFERENCE ON CYCLOTRONS AND THEIR APPLICATIONS
Bloomington, IN, September 18-21, 1978

CHARGE EXCHANGE LOSSES DURING CYCLOTRON ACCELERATION: EXPERIMENT AND THEORY

R. A. Gough* and M. L. Mallory**

Abstract

Quantitative estimates of charge exchange (CE) losses during acceleration are very important in the design and operation of heavy ion cyclotrons. Such estimates have been made using a vacuum model computer code which was developed to establish vacuum requirements for the MSU superconducting heavy ion cyclotron. This code uses pressure and cross-section data to calculate the radial loss of beam due to charge exchange. Since CE cross sections and radial pressure profiles are not always well known, certain specific measurements have been made using the LBL 88-Inch Cyclotron to provide experimental data needed to test the code. These include measurements of pressure versus radius under vacuum conditions closely approximating those existing during acceleration of $^{14}N^{4+}$ and $^{40}Ar^{8+}$ beams. Beam intensity versus radius data demonstrating transmission losses for three beams are presented. Comparisons with theoretical predictions are given.

Introduction

The vacuum requirements for heavy ion acceleration in cyclotrons in the past have depended primarily upon the experimental measurements of beam attenuation data and the associated problems of data interpretation. A preferable approach is the construction of a theoretical model that calculates the necessary vacuum requirements for any beam desired. In recent years, advances in theory and experimental measurements of charge exchange loss cross sections have made it possible to construct such a vacuum model for heavy ion cyclotron acceleration. However, many simplifying assumptions are made in the model and a check upon the model validity versus the experimental beam attenuation results is required. The following sections contain a brief outline of the vacuum model, experimental descriptions of the 88-Inch Cyclotron equipment used for vacuum measurements, followed by comparison of calculated attenuation losses with experimental results observed on the 88-Inch Cyclotron in Berkeley.

Heavy Ion Vacuum Model

Transmission of a heavy ion beam through a cyclotron is generally described by the function $\exp(-\sigma px)$ where σ is the charge exchange cross section, p is the pressure and x is the path length. The CE losses for heavy ion acceleration are composed of charge pickup and charge stripping processes (i.e. $\sigma = \sigma_p + \sigma_s$). The charge pickup process dominates at low energy. No theoretical model of charge pickup cross section as a function of energy (relevant to cyclotrons) exists. Recently Olson and Salop[1] have developed theoretical equations for charge pickup at very low energy, i.e. essentially zero energy for cyclotrons. Another cross section data point for charge pickup can now be obtained from a different kind of experimental data. Namely, Betz[2] has derived an empirical equation for relating the energy at which the accelerated ion of charge q is in equilibrium with the charge pickup and charge stripping processes. Hence, at that energy the charge pickup cross section is equal to the charge stripping cross section and this value can be obtained from the Bohr-Leinhardt equation.[3] It is then assumed that the pickup cross section between these two points is given by $\sigma_p(E) = \sigma_p(E=0)\, e^{-\gamma E}$, where σ_p is the pickup cross section, E is the energy, γ is the constant for the two pickup cross section points described above. Examination of experimental cross section data with this assumption reveals good agreement.

The charge stripping cross section has used the Bohr-Leinhardt equation,[3] with the loss cross section set constant after the ion velocity exceeds the outer electron velocity of the accelerated particle. An example of the cross section calculated from this model is shown in Figure 1(a) for $^{238}U^{12+}$.

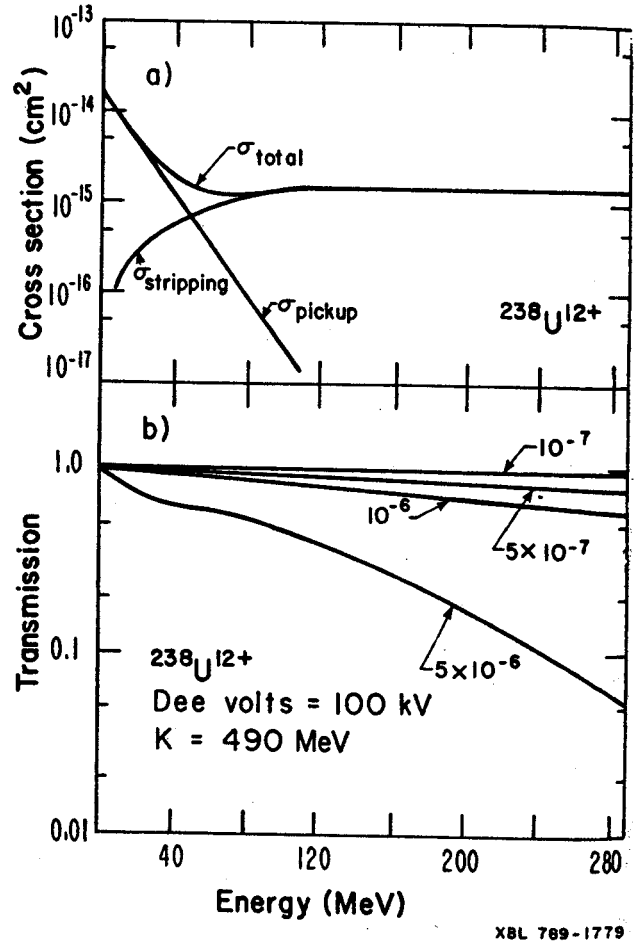

Fig. 1. a) The theoretical loss cross section for $^{238}U^{12+}$ is shown. It is composed of a low energy portion due to charge pickup, and a high energy portion due to charge stripping. b) The transmission of $^{238}U^{12+}$ through a K = 490 MeV, 3-dee cyclotron is shown for various pressures. Greater than 90% will be transmitted for a pressure of 10^{-7} Torr.

* Present address: Lawrence Berkeley Laboratory Berkeley, California 94720
** Present address: Michigan State University East Lansing, Michigan 48824

0018-9499/79/0400-2384$00.75©1979 IEEE

PROCEEDINGS OF THE 1979 PARTICLE ACCELERATOR CONFERENCE, San Francisco, CA, March 12-14, 1979

PROGRESS REPORT ON THE 500 MEV SUPERCONDUCTING CYCLOTRON*

H. Blosser and P. Resmini
Cyclotron Laboratory, Michigan State University
East Lansing, MI 48824

Summary

The 500 MeV first stage of an eventual two stage superconducting cyclotron system is in the final year of its construction phase. Major design features of the overall coupled system and construction status of the 500 MeV first stage cyclotron are reviewed.

Text

The MSU Cyclotron Laboratory is in the process of designing and constructing a large double cyclotron system[1] for the purpose of providing high quality beams of heavy ions with energies up to 200 MeV per nucleon for lighter heavy ions such as calcium and up to 20 MeV per nucleon for the heaviest particles such as uranium. Fig. 1 graphically depicts the goals of the project in terms of intensity contours vs. energy per nucleon and mass number. The operating range reaches well above the Coulomb barrier which is indicated by the lower solid lines in the figure for the two cases of identical projectile and target (A→A) and for a projectile of mass number A bombarding uranium (A→U). The operating range for essentially all projectiles also reaches above the expected onset of "sonic" or compressional wave phenomena in nuclei expected at around 20 MeV per nucleon and reaches into the region of coherent meson production and doubling of the nuclear density for a substantial number of lighter projectiles.

Fig. 2 is a schematic drawing showing major functional features of the coupled cyclotron system. Ions from a conventional cold cathode ion source are accelerated through approximately 100 turns in a first-stage superconducting cyclotron and are then extracted. These ions, with energy $E_1 = K_1 Q_1^2/A$, where K_1 is the energy parameter of the cyclotron (500 MeV at full field), Q_1 is the charge of the ion in units of the electron charge, and A is the mass of the ion in atomic mass units, are then transported in an isochronous transfer line and directed into the center of a second larger cyclotron with a nominal 800 MeV energy parameter. The beam direction is adjusted such that, taking account of the curvature of the ion as it passes into the field of the cyclotron, the orbit will finally arrive at a point where it is just tangent to a centered equilibrium orbit with length 1/3, 1/4, 1/5... of the length of the final extraction orbit in the previous cyclotron. A stripping foil placed at this point of tangency between the injection orbit and the innermost equilibrium orbit of the second cyclotron gives a charge change from a typical value of ≈ 8 to a typical value of ≈ 25. The magnetic field of the second cyclotron is set so that the rigidity of the after-stripping charge state matches the design rigidity of the injection orbit; the ion is therefore captured on this orbit and thereafter accelerated. Finally the beam is extracted from the second cyclotron and directed into a transport system which feeds to an array of experimental devices.

Fig. 3 gives a vertical section view of the first stage 500 MeV cyclotron and shows the general arrangement of major components. The superconducting element of the cyclotron is the main coil, a large solenoid-like coil of average diameter 65.5" and overall height approximately 40". The active winding of the coil divides into symmetric halves relative to a 3" median plane gap at the mid-height point. The winding on each side of median plane is further subdivided into a "small coil" close to the median plane and a "large coil" further away from the median plane with the mirror sections on each side of the median plane wired in series to preserve symmetry. The small coil and large coil sections are, however, independently powered and the different radial form factors of these coils (the small coil field rises with radius by approximately 15% relative to the central value, whereas the large coil field is practically flat) are used as the primary field shaping element to accomplish the isochronous matching required for ions of differing mass and energy.

Cooling for the main coil is provided by a conventional helium bath immersion system. The coil is housed in an annular cryostat with a 52" diameter warm bore and conventional room temperature components of the cyclotron are inserted from top and bottom in this warm bore. Where necessary, room temperature penetrations pass through the median plane slab of the coil for items such as beam extraction, electrostatic deflector power leads and supports, probes, etc. (Reentrant vacuum liners are provided for all of the median plane penetrations so that the insulating vacuum of the coil is entirely independent of both cyclotron and beam line vacuums and therefore safe from disruption by possible vacuum accidents in either of these systems.)

The radio frequency system[2] for the cyclotron is a "dee-in-valley" design with a dee in each of three valleys, each dee being electrically designed as a half wave resonator, i.e. with a quarter wave coaxial line tuning stub on both top and bottom. The broad range of charge to mass ratios involved in the design operating range (from 1/2 for the lightest ions to 1/40 for the heaviest ions) translates into a desire for a broad tuning range in the radio frequency system, namely from 9 MHz to 32.4 MHz (a smaller range could be used but would require greater use of harmonic acceleration with considerable degradation of beam quality). Each of the three dees is driven from an independent power amplifier with phasing circuits allowing relative phasing of the dees to be set at 0°, 120°, and 240°. With such a "three-phase" system, acceleration on all harmonics (where the "harmonic" number is the ratio of the rf frequency to the orbital frequency) is in principle possible and use of harmonic numbers 1, 2, 3, 4, 5, and 7 is contemplated in covering the design operating range.

The three rf power amplifiers which drive the dees are located approximately 10' from the cyclotron in corner positions in the shield enclosure. Fig. 4 is a schematic drawing of the arrangement. The transmitter includes an impedance matching system consisting of an inductive coupling loop and a quarter wave resonant line constructed in a fashion similar to the dee stem. The main amplifier tube is a 4CW100,000 tetrode. Fig. 5 is an electrical circuit diagram for the rf system showing various tuning circuits and the single-sideband heterodyne tuning logic.

Beam extraction[3] is accomplished by two electrostatic deflectors of conventional design coupled with a series of inert magnetic elements called "focusing bars". These latter consist of sets of three iron bars arranged in a manner suggested by Hoffmann[4] which gives a combined dipole and quadrupole field component of good strength. Optical characteristics of the extraction system have been numerically studied over the full operating range of the machine; results show excellent beam characteristics. In particular, the

PROCEEDINGS OF THE 1979 PARTICLE ACCELERATOR CONFERENCE, San Francisco, CA, March 12-14, 1979

LIFETIME IMPROVEMENTS OF HEAVY ION SOURCE CATHODES*

P.S. Miller, H. Laumer, M.L. Mallory, and J.A. Nolen

Cyclotron Laboratory, Michigan State University, E. Lansing, MI 48824

Abstract

The cathode lifetime for a cold cathode Penning heavy ion source has been increased to ≈24 hrs. (a factor of 7 increase) by the use of hafnium cathodes when accelerating a carbon beam on the Michigan State University cyclotron. Compared to tantalum, the hafnium cathodes are operated at reduced power (≈2 kW) to avoid melting them. Thus, while the carbon beam intensity achieved with Ta cathodes is 3 to 10 times higher than that from the Hf cathodes, this is no advantage for experiments which need low beam currents (e.g. due to count rate limitations). For injection into a K=800 cyclotron the higher intensity for lower charge states from a lower power source is expected to favor Hf cathodes. Lowering the arc power for Ta cathodes, thus reducing beam intensity, does not substantially lengthen cathode lifetime. Source feed gas composition strongly influences Hf cathode performance. Extended lifetimes were achieved with CO while Ne gas resulted in very short lifetimes, suggesting the difference may be due to a chemical reaction between the Hf cathodes and an element in the feed gas.

Introduction

Positive heavy ion sources are used in most major heavy ion accelerators. For isochronous cyclotrons, the final energy of the projectile depends upon the square of the ion charge state (q^2) and therefore maximum energy experiments stress the production of high charge state ions and thereby require maximum source performance. Another class of experiments runs at energies and intensities that are easily met by present sources. The curve labeled K500 in Fig. 1 defines a boundary in energy per nucleon vs. mass for the K500 cyclotron, now under construction at Michigan State University,[1] where source intensity is not the limiting factor. Fig. 1 also contains the energy per nucleon curve for the K500-K800 coupled cyclotron (with 3 to 1 stripping) that is under design at Michigan State University[2] and delineates a larger region where source intensity is not limiting performance. Both regions cover a significant fraction of the expected operating range of the accelerator performance curve.

The present method for reducing cyclotron heavy ion source intensity is to increase the source gas flow. No additional benefits to ion source operation are gained from this mode of source operation. In the following section is described a series of experiments with a $^{12}C^{4+}$ beam on the K58 Michigan State University cyclotron. Increased source lifetime was achieved at the expense of reduced beam intensity; however, this was a significant improvement of performance for the experiments in question.

Ion Source Lifetime Experiments

The lifetime of a positive ion source depends upon various factors (e.g. duty cycle, gas, cathode material). Various materials have been tried as cathodes, but predominantly tantalum or tungsten cathodes have superior beam performance and are used in most cyclotron sources. At Michigan State, it was observed that hafnium targets were difficult to make by sputtering and it was suggested that hafnium be tried as cathodes in the heavy ion source.

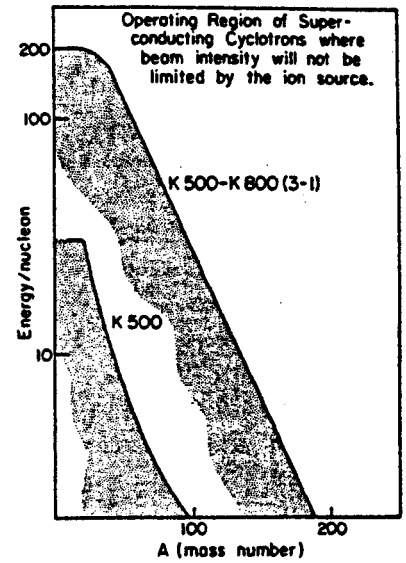

Fig. 1. The energy per nucleon is shown vs. mass for the K500 cyclotron and the coupled K500-K800 cyclotrons (with 3 to 1 stripping) where the particle beam intensity will not be limited by the ion source. The shaded region covers a large fraction of the expected operating range and in this region the beam intensity can be traded for improved ion source lifetime.

Lifetime experiments using hafnium cathodes and an internal cyclotron carbon beam were performed yielding a significant improvement in ion source lifetime (> 24 hours for two sources). The hafnium cathodes were then used in a nuclear physics experiment. It was found that compared to tantalum, hafnium cathodes would melt at lower arc power and as a result the intensity of on target beam was diminished. The cathode lifetime, however, was increased. A series of experiments were then performed to compare lifetimes and beam intensities of tantalum and hafnium cathodes. Tables I and II are the results of these experiments and show that the intensity for the hafnium cathodes when using CO gas was ≈ 10 times less than achieved with tantalum cathodes, but the lifetime for the hafnium cathodes was much greater. The best arc parameters for the hafnium cathodes were determined to be 2 amp and 1000 volts, where additional arc current can result in melting the cathodes. Experiments using neon gas and nitrogen gas with hafnium cathodes resulted in short lifetimes and thereby suggested that the lifetime improvement was associated with some surface reactions on the cathodes between hafnium and the carbon monoxide source gas.

Cathodes containing pressed hafnium carbide and hafnium oxide were developed (see Fig. 2) and then run in an ion source test stand, using nitrogen source gas. It was determined that hafnium carbide cathodes resulted in long lifetimes and hafnium oxide in short lifetimes. A set of hafnium carbide cathodes were then run on the cyclotron and produced a long lifetime, but were very unsatisfactory, since the beam intensity was erratic. This erratic operation is

FIRST INTERNATIONAL SYMPOSIUM ON MICROBIAL ECOLOGY, DUNEDIN, NEW ZEALAND, August, 1977

Short-Term Measurement of Denitrification Rates in Soils Using ^{13}N and Acetylene Inhibition Methods

J.M. TIEDJE, M.K. FIRESTONE, M.S. SMITH, M.R. BETLACH, and R.B. FIRESTONE

A. Introduction

Denitrification has long been recognized as a basic component of the nitrogen cycle: it results in the loss of combined nitrogen, a limiting nutrient for primary productivity. Though the importance of this loss to agricultural and natural ecosystems is well known, denitrification remains the least understood transformation in the nitrogen cycle. In addition there has been recent concern about the denitrification intermediates, N_2O and NO_2^-. The former catalyses destruction of the ozone layer through its photochemical product NO and the latter reacts with secondary amines to form nitrosamines which are potent carcinogens. There has been much recent interest also in use of denitrification to rid waste products of excessive nitrogen. Despite the general significance of this process, research progress has been limited because of the absence of direct, sensitive, and precise methodology to assay denitrification in nature.

We have used two new and complementary methods which overcome this previous methodological limitation. One method employs the radioactive isotope of nitrogen, ^{13}N, because of the greatly improved sensitivity it provides. The specific activity is 1.04×10^{12} mCi/g-atom which provides a minimum detectable amount of 3×10^{-14} µmoles. The other uses acetylene to inhibit N_2O reductase thereby causing stoichiometric accumulation from nitrate of nitrous oxide, which can be easily measured by gas chromatography (1, 4). In this paper we report on the evaluation of and information obtained from the use of these two methods to measure rates and products of denitrification in fresh soils.

B. Materials and Methods

1. ^{13}N. ^{13}N has a half-life of 10 minutes, emits positrons (1.19 MeV) which, upon annihilation, formed two 0.511 MeV gamma rays. We generate $^{13}NO_3^-$ at the MSU Sector Focused Cyclotron by using 0.7 ml of water as the target, employing the $^{16}O(p, \alpha)^{13}N$ reaction. We used a 0.7 to 4 µA, 11.5 to 14.5 MeV proton beam bombarding for 10 minutes. A pneumatic rabbit is used to transport the target in and out of the beam. The nitrogen composition of the product is >80% nitrate with lesser quantities of nitrite and ammonium present. The latter two contaminants can be removed by oxidation and volatilization respectively.

Soils were incubated in either sealed flasks or flasks in which soil slurries were constantly flushed with helium. The latter incubation system and its subsequent gas collection and detection system are shown in Figure 1. The $^{13}NO_3^-$ (~1 mCi, 4.4 pg) with or without $^{14}NO_3^-$ carrier was added to the soil slurry which was mixed by a magnetic stirrer and continuously stripped of product gases with helium. The flushed gases passed first through a trap which consists of tubing immersed in liquid nitrogen, and subsequently through a second trap which consists of tubing packed with Molecular Sieve and immersed in liquid nitrogen (2). The detectors are NaI crystals attached to photomultiplier tubes. The data are continuously

In Microbial Ecology, (eds) M. W. Loutit and J. A. R. Miles, Springer-Verlag, Berlin.

PROCEEDINGS OF A SYMPOSIUM HELD AT THE GODDARD SPACE FLIGHT CENTER, GREENBELT, MD, April 28-29, 1978

Cross Sections Relevant to Gamma Ray Astronomy†

P. Dyer

University of Washington, Seattle, WA 98195
and
Michigan State University, East Lansing, MI 48824

D. Bodansky

University of Washington, Seattle, WA 98195

D.R. Maxson

University of Washington, Seattle, WA 98195
and
Brown University, Providence, RI 02912

We have measured gamma-ray production cross sections relevant to gamma-ray line astronomy for protons and alpha particles incident on targets consisting of nuclei of high cosmic abundance: ^{12}C, ^{14}N, ^{16}O, ^{20}Ne, ^{24}Mg, ^{28}Si, and ^{56}Fe.

Solid or gaseous targets were bombarded by monoenergetic beams of protons and alpha particles, and gamma rays were detected by two Ge(Li) detectors. The proton energy for each target was varied from threshold to about 24 MeV (lab); for alphas the range was from threshold to about 27 MeV. For most transitions, it was possible to measure the total cross section by placing the detectors at 30.5^{o} and 109.9^{o}, where the fourth-order Legendre polynomial is zero. For the case of the ^{16}O (E_{γ} = 6.13 MeV, multipolarity E3) cross sections, we measured yields at four angles. Absolute cross sections were obtained by integrating the beam current and by measuring target thicknesses and detector efficiencies. The Ge(Li) detector resolution was a few keV (although the peak widths were greater, due to Doppler broadening).

An overview of the measured gamma-ray cross sections for incident protons is presented in Fig. 1, where the cross section and energy of the most prominent gamma-ray line for each target are displayed for several proton energies. Except for ^{16}O, these lines correspond to the de-excitation of the first excited state of the target nucleus; for ^{16}O the transition is from the second excited state to the ground state. If the energy spectrum of the interacting particles is known, the cross sections can be used to deduce relative nuclear abundances at the gamma ray source. The abundance analysis will be somewhat complicated by the multiplicity of channels opened up as the incident energies increase. For example, for protons above about 13 MeV, the 4.44-MeV gamma rays from the first excited state of ^{12}C can be produced in the $^{16}O(p,p\alpha)^{12}C$ reaction, as well as in the $^{12}C(p,p')^{12}C$ reaction.

The multiplicity of lines from a given target can also be useful. Of special interest are cases where the different gamma-ray lines have different excitation functions, for example the 0.847-MeV gamma rays produced in $^{56}Fe(p,p')^{56}Fe$ reactions and the 0.812-MeV gamma rays produced in $^{56}Fe(p,n)^{56}Co$ reactions. The relative yield in such cases can provide insight into the energy spectra of the interacting particles.